REPORT





Fence Springs of the Grand Canyon, USA: insight into the karst aquifer system of the Colorado Plateau region

Chris McGibbon¹ · Laura J. Crossey¹ · Karl E. Karlstrom¹

Received: 23 July 2021 / Accepted: 3 September 2022
This is a U.S. Government work and not under copyright protection in the US; foreign copyright protection may apply 2022

Abstract

Fence Springs are the highest discharge springs of the Redwall-Muav (R-M) karst aquifer in Marble Canyon of eastern Grand Canyon, Arizona, USA. Vents on opposite banks of the Colorado River within the Fence fault system have similar chemistries indicating the springs are connected hydrologically within the confined karst aquifer below the river. Stable isotope data fingerprint the recharge area for both springs to be the Kaibab Plateau, west of the river. Chemical variation in nearby R-M springs indicates mixing between karst base flow (represented by Fence Springs) and fast-traveled meteoric waters (Vasey's Paradise). A 7-year record (2012—2019) suggests the karst base flow has steady temperature (~20 °C) and specific conductance (~2,000 μS/cm) and no seasonality. A progressive decrease of ~1 °C in both springs and ~100 μS/cm in Fence East over 7 years reflects declining spring discharge accompanying declining meteoric recharge. Fortuitous high-flow experiments in the Colorado River during Glen Canyon Dam management operations provide data analogous to a "slug test" for the groundwater system. Rapid increase in river level from ~142 to 1,218 m³/s caused the springs to be inundated and mix with river water. Recovery curves showed rapid return of spring temperature from ~10 to 20 °C and specific conductance from 500 to 2,000 μS/cm once river stage fell below ~283 m³/s. After 2016, an increase in short-term fluctuations during recovery suggests declining spring discharge through the 7-year period. This multitracer hydrochemical dataset combined with spring monitoring helps establish a baseline for groundwater in eastern Grand Canyon.

Keywords Springs · Karst · Groundwater monitoring · Time series · Multiple permeability · USA

Introduction

Grand Canyon provides a cut-away view (>1 km deep) of the hydrogeologic system of the Colorado Plateau region, USA. Groundwater in the eastern Grand Canyon region is recharged mainly from the ~2,500-m-elevation Kaibab Plateau and discharged in major springs within Grand Canyon (Huntoon 2000; Fig. 1a). Two important examples include Roaring Springs, the major water supply source for both the North and South Rim Park developments, and Fence Springs, the major spring system in Marble Canyon and the subject of this study (Fig. 1b). The goals of this study are to examine the mixing

Published online: 18 October 2022

of different waters within karst-fed springs east of the Kaibab uplift and provide a current (2022) baseline understanding of groundwater in the Redwall-Muav (R-M) aquifer of Marble Canyon.

Figure 1a summarizes the results of a dye tracer study where dyes were injected into sinkholes on the Kaibab Plateau and detected at distant springs, documenting long-distance fast recharge to major springs along complex fault-related fluid pathways (Jones et al. 2018). Fence Springs (Fig. 1b, c) is an important occurrence because this spring system reflects the majority of the water discharging east of the Kaibab uplift within Marble Canyon and its different spring compositions can be used to parse the mixing of different water sources, and pathway complexities. This article reports on natural hydrochemical tracers for springs of the Fence Springs system and compares these data to Roaring Springs and Bright Angel Creek, which discharge on the south side of the Kaibab uplift (Fig. 1a).



Chris McGibbon mcgibbon@unm.edu; cjmcgibbon@outlook.com

Department of Earth and Planetary Sciences, University of New Mexico, Albuquerque, NM 87131, USA

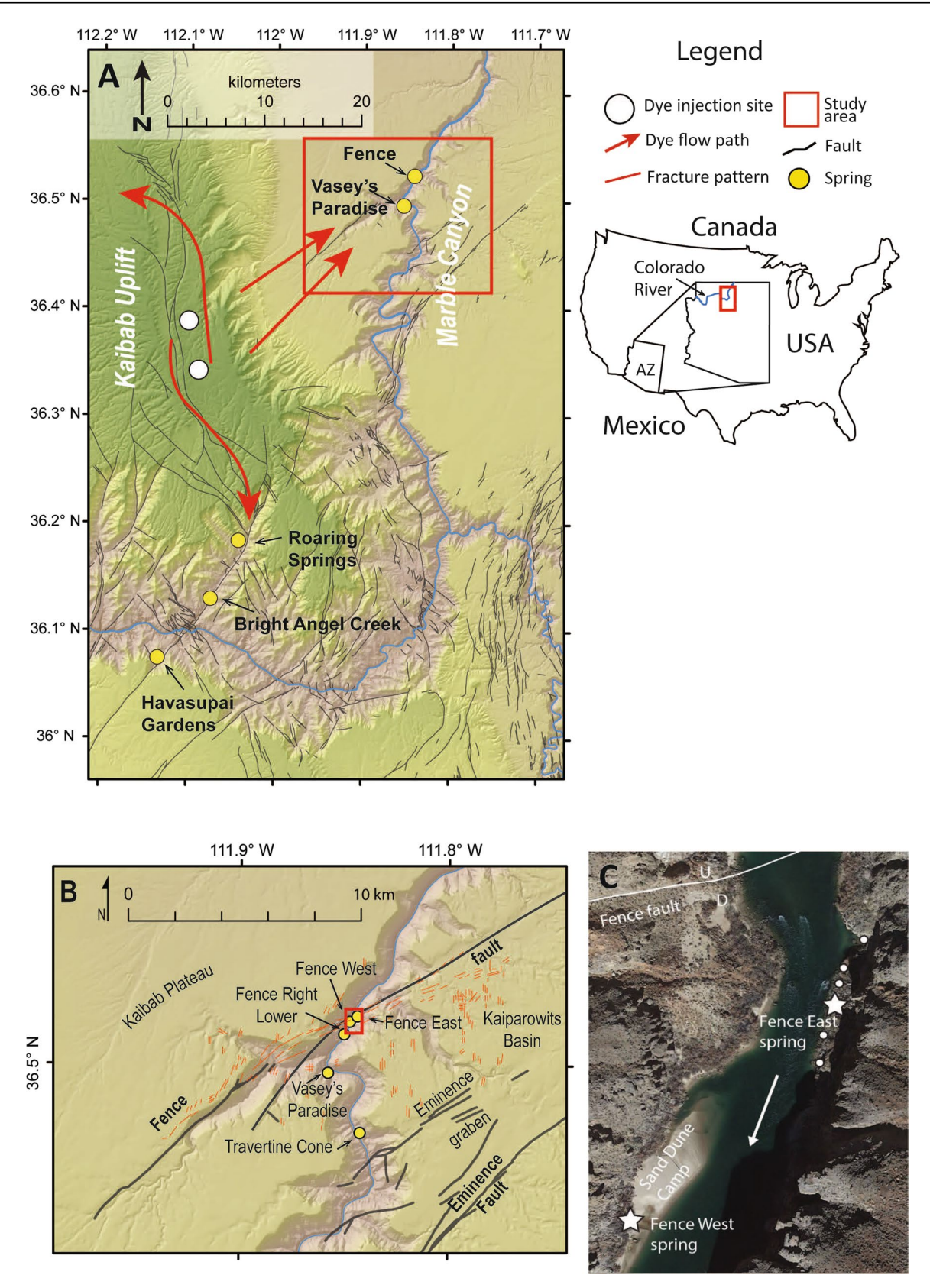


Fig. 1 Springs and faults of the Fence fault area of Marble Canyon. a Location relative to Kaibab uplift with white dots showing injection locations for dye tracers that arrived within a year at Vasey's Paradise (Jones et al. 2018). b Fence Springs system within Eminence graben

and related normal faults (black, from Billingsley and Hampton 2000) and dominant fractures (red, from Google Earth). **c** Detail of Fence East and Fence West main springs (stars) and subsidiary springs (dots) on Google Earth image

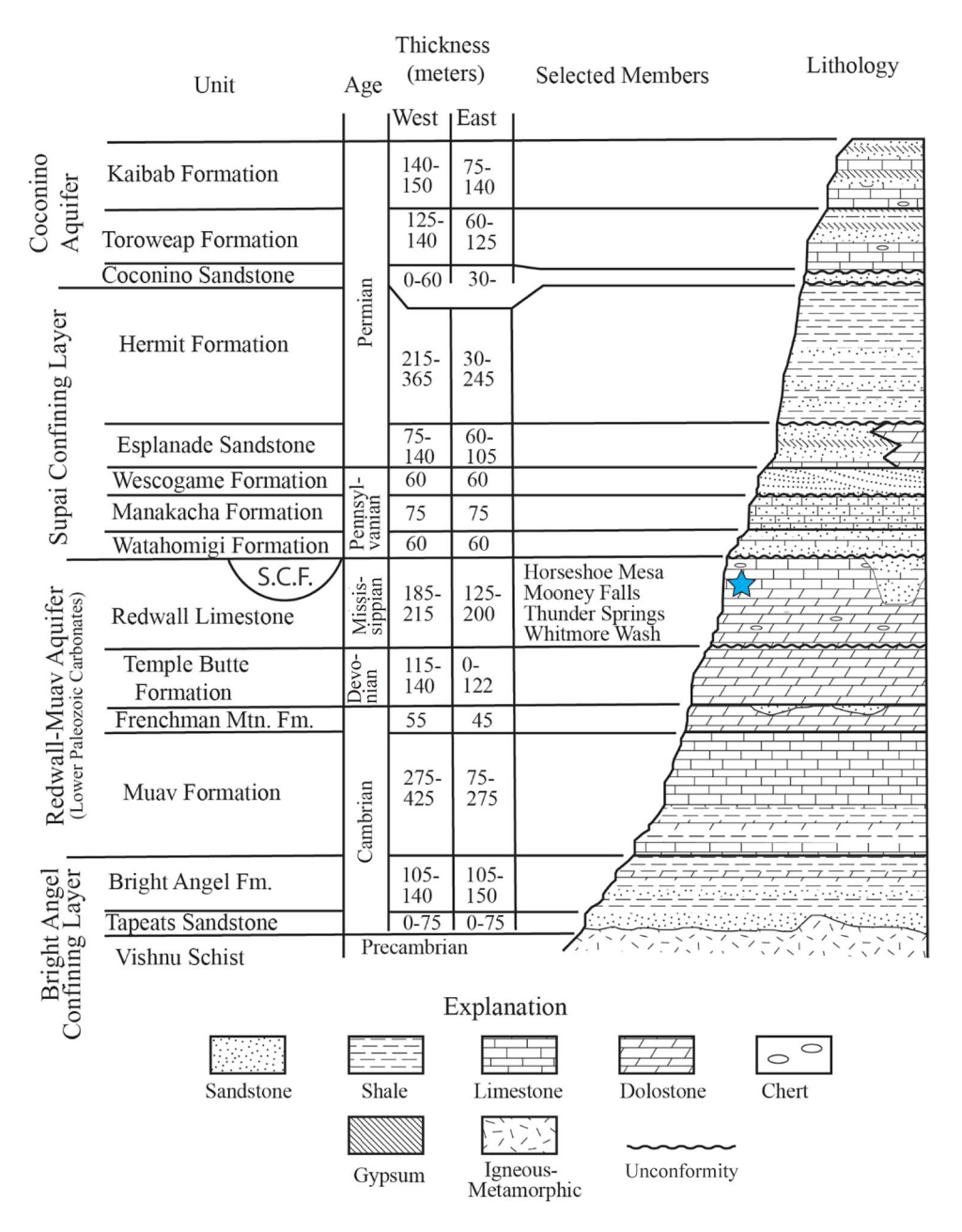


Figure 2 shows the stacked sedimentary aquifers of the Colorado Plateau (Huntoon 2000) that include the Redwall-Muav (R-M) karst aquifer, the mixed karst-sandstone aquifer of the Coconino aquifer (C-aquifer), and fault networks that allow vertical connectivity between aquifer units. The R-M aquifer discharges the vast majority of groundwater in Grand Canyon. The hydrogeology of the R-M aquifer remains incompletely characterized in part because there are few deep wells and limited geophysical surveys on the rim regions adjacent to the Grand Canyon (Bills et al. 2016; Jones et al. 2018).

Fence Springs system in Marble Canyon (Fig. 1b,c) is a unique example of a high-discharge artesian spring system, located along a normal fault system, which discharges from

the R-M aquifer on opposite banks of the Colorado River. It was first studied in detail by Huntoon (1981), who suggested that the springs on the east and west sides of the river are hydrologically and geochemically connected with each other, but not with the river, thus providing a case study of numerous karst aquifer characteristics. Huntoon (1981) noted that during high river stages, spring discharge still occurred, as evidenced by warmer water around the springs, and that spring temperatures remained constant, indicating that river water did not enter the fault zone. He interpreted the different chemistries of the subsidiary springs to reflect mixing between two end members, one represented by Fence East and the other by Fence West Lower (Fig. 1b; his Diagonal Spring) that had different depths of circulation in the confined karst aquifer

Fig. 2 Paleozoic rocks and hydrostratigraphic units of the Grand Canyon region of the Colorado Plateau (modified from Huntoon 2000). Blue star is the stratigraphic level of the Fence Springs system





(Fig. 3). The different chemistry of Vasey's Paradise Springs, about 2 km downriver (Fig. 1b), was interpreted to reflect a partially independent flowpath from the Kaibab uplift.

Huntoon (2000) proposed a general hypothesis for dual permeability flow with two main flowpaths: (1) unconfined high gradient cave and fault conduits carrying fast-traveled meteoric recharge; and (2) confined low gradient 3D mazes of fractures with steady flow, high storage, and significant water-rock interaction, hence higher total dissolved solids (TDS). This concept was amplified by Crossey et al. (2006, 2009) who identified an additional hydrochemical component: geochemically potent small volume endogenic (deeply sourced) hydrothermal fluids that ascend along faults and contain high CO₂, high TDS, and mantle-derived ³He. These endogenic fluids interact with the large volume R-M aquifer (No. 2 preceding), which is carbonic and warm due mainly to long flow paths as well as potential geothermal input. Recent dye tracer studies on the Kaibab uplift (Fig. 1a) help quantify the fast-traveled meteoric component for snowmelt and monsoonal events moving through sink holes and unconfined fault and cave conduits into the R-M aquifer (Tobin et al. 2017; Jones et al. 2018).

Here, the interrelationships between multiple permeabilities and multiple hydrochemistries in the Grand Canyon hydrologic system are explored by analyzing natural hydrochemical tracers in the Fence Springs system. The authors summarize 17 years of campaign sampling and add major ion analyses, stable isotope geochemistry, and continuous monitoring data (depth, temperature, and specific conductance). These data reinforce the overall conclusions of a confined fault-related aquifer system that connects the springs beneath the river (Huntoon 1981), but new stable isotope data indicate that springs on both sides are sourced predominantly from the Kaibab Plateau west of the Colorado River. Other R-M springs within a few river miles (~4–5 km) of the Fence Springs are shown here to be hydrochemically distinct because of mixing additions of fast and flashy (unconfined) conduit-flow waters

into the slow and steady base flow (confined) groundwater residing in the R-M karst system of Marble Canyon.

Autonomous sensor technologies were also applied to look at changes through time at these springs over the past 7 years, and sensors were installed in 2012 that recorded semicontinuous temperature, depth, and specific conductance data from 2012–2019. This time period is long enough to begin to see temporal trends that may be of regional importance and to help distinguish temporal trends from mixing trends in the aquifers. During this time, there were several high-flow experiments (HFEs). These were large releases from Glen Canyon Dam, up to 43,000 cubic feet per second (cfs; 1,218 m³/s), designed to refine dam management and ecosystem sustainability protocols, that have also provided a fortuitous set of multimillion-dollar slug test experiments to evaluate the R-M karst aquifer.

The combined use of natural and anthropogenic tracers with continuous spring monitoring is also needed in other spring systems of Grand Canyon to establish a long-term hydrologic base line for the region. Both water supply and water quality are major concerns due to increases in visitation to Grand Canyon Village, growth of local towns such as Tusayan and Valle (Fig. 1), uranium mining, and development schemes (Adams 2005; Bills et al. 2016; Tillman et al. 2020).

Study area

Geology and regional hydrology

Figure 4 shows a schematic diagram of the hydrogeologic setting of the Fence Springs system in eastern Grand Canyon. Four hydrochemical waters are shown to mix in the aquifer system (Crossey et al. 2006). Firstly, the Colorado River, is sourced by snowmelt in the Rocky Mountains and is hydrochemically distinct from local springs and groundwaters; additionally, it is cold (10 °C) because it emerges from the

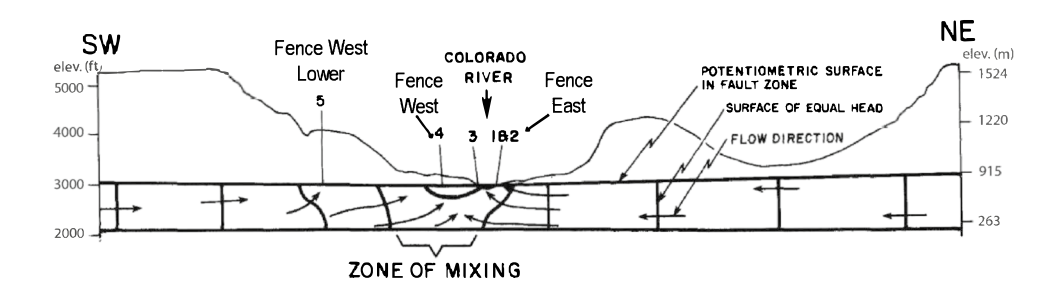
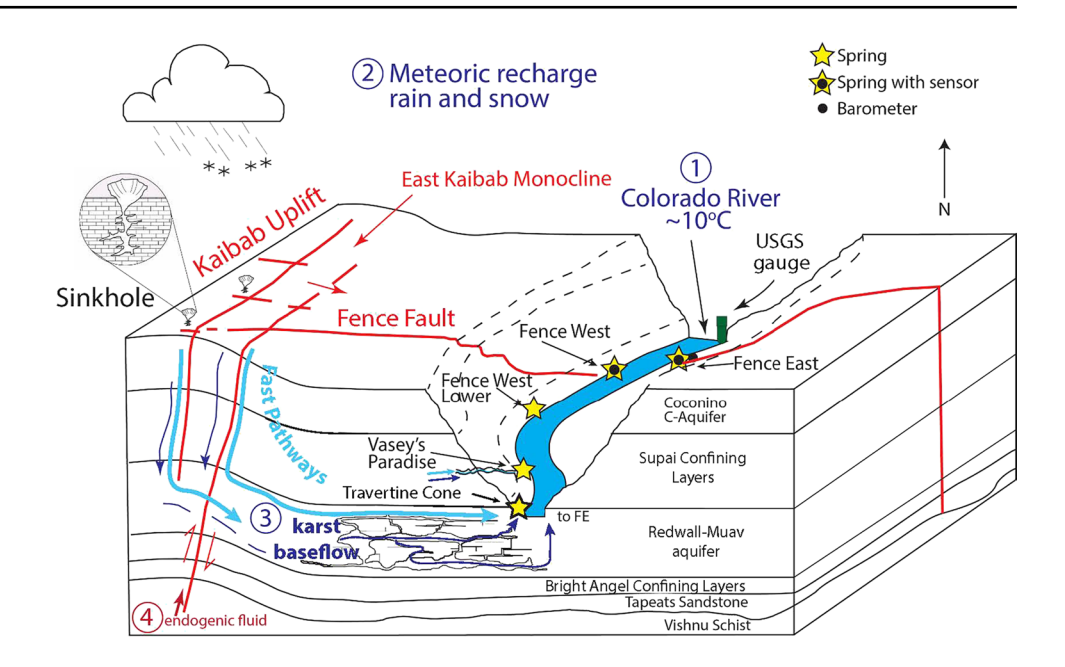


Fig. 3 SW–NE fault-parallel cross section showing the assumed circulation system and spring connection beneath the Colorado River (modified from Fig. 6 of Huntoon 1981). Numbers refer to Huntoon's numbering of springs: Nos. 1–2 = Fence East (FE) in this study, 4 = our Fence West (FW) location, No. 5 = our Fence West Lower loca-

tion (Huntoon's Diagonal Spring). Huntoon (1981) concluded that water flowed from east to west; the authors of this study conclude from stable isotope data that water flows from west to east and both Fence East and Fence West are derived from the Kaibab Plateau to the west



Fig. 4 Block diagram showing springs investigated in this report. The main flow paths from the Kaibab uplift recharge area are interpreted to be downward along faults and canyonward in the R-M karst aquifer. Circled numbers refer to water mixing components to be evaluated: (1) Colorado River (T~ 10 °C), (2) snow and rain recharge from the high elevation Kaibab uplift ($T \sim 0-10 \,^{\circ}\text{C}$), (3) R-M aquifer base flow ($T \sim 20$ °C), (4) small volume but geochemically potent endogenic fluid. The base of the active groundwater circulation is assumed to be shales of the Bright Angel Formation confining layer



base of Lake Powell at Glen Canyon Dam. Secondly, meteoric recharge from the Kaibab uplift finds its way down via fast pathways in faults and caves through the different aquifers (Huntoon 1981). Thirdly, karst base flow in the R-M karst aquifer has the region's largest volume of storage and has a mixture of all the fluid components; groundwater moves slow enough through the karst fracture systems to equilibrate with rock and emerge at Fence Springs at ~20 °C (Huntoon 2000). Fourthly, small volume but geochemically potent carbonic fluids ascend along faults as shown by trace gas studies that reveal mantle ³He, significant deeply sourced CO₂, and a variable geothermal temperature addition (Crossey et al. 2006, 2009). The resulting complex mixture of different fluid chemistries at a given spring or well, and in different parts of the R-M aguifer, depends on incompletely known end member fluid compositions and volumes within the different permeability pathways.

Recharge areas for the deep R-M aquifer regionally includes the high elevation uplands both north and south of Grand Canyon. Groundwater from the adjacent plateaus flows towards Grand Canyon, the hydrogeologic sink in the area (Monroe et al. 2005). The Kaibab Uplift north of Grand Canyon is of the most importance for the Fence Springs system (Huntoon 1981). Water infiltrates the C-aquifer in the high elevations of the plateau and descends through dissolution-enhanced faults, fractures and sinkholes (Huntoon 1974, 2000; Kessler 2002). Monsoonal events can lead to rapid changes in discharge, temperature and specific conductance in the unconfined parts of the karst systems, whereas these events are dampened in the confined basin karst systems, in some cases, to the point where they may not even be recognized (Huntoon 2000; Jones et al. 2018).

Groundwater from the Kaparowitz hydrologic basin (Cooley et al. 1969) to the east of Marble Canyon was considered important by Huntoon (1981) but is not a major source for Fence Springs, as discussed in the following.

Overall, the Paleozoic sedimentary strata of Grand Canyon have relatively low permeability and hydraulic conductivity, due in part to the stratigraphy being primarily fine-grained, mudstone and sandstone, limestone and dolomite, as well as the confining nature of the alternating rock types (Bills et al. 2007; Crossey et al. 2006; Jones et al. 2018). As a result, faults, fractures, and folds play an important role in the infiltration and transportation of groundwater (Kessler 2002). The faults and fracture zones can act as conduits, providing lateral and vertical planes of increased permeability in areas with typically low hydraulic conductivity. The increased vertical permeability provides hydraulic continuity across confining beds within the upper Paleozoic section and serves to connect the plateau surface with the aquifers (Metzger 1961; Huntoon 1981). Shales of the Bright Angel Formation form the major lower confining layer for the R-M aquifer.

Fence fault system

Fence fault is the northwestern fault system bounding the Eminence graben, a 10-km- (~6-mile) wide graben bounded on the southeastern side by the Eminence fault (Fig. 1b). Both Fence and Eminence faults are high-angle normal faults, with displacement ranging up to 76 m (Huntoon and Sears 1975). The Eminence graben (Fig. 1b) is pervasively fractured by vertical joints in the inter-fault areas and this permeability increases groundwater circulation through the down-dropped blocks (Lange 1956). The result is joint-controlled caves in



the carbonates which are seen up to 50 m high on the canyon walls. The main modern groundwater flow that makes use of these ancient circulation systems are in the Fence Springs system (Huntoon 1981).

Fence fault of the eastern Grand Canyon has multiple springs that discharge near the fault zone along subsidiary fractures and through karst breccias in the Redwall limestone on either side of the river (Fig. 4). Spring vents are in the fracture network of the river-crossing Fence fault, on its downthrown side, not along its main strand. Fence East Springs (441 L/s; ~0.44 m³/s; 15.5 cfs) is artesian and emerges at the edge of the river; it is emergent at low river stage (<283 m³/s; 10,000 cfs; Fig. 5a) and covered at higher river stages. Fence West Springs have lower flow (57 L/s; 0.06 m³/s; 3 cfs) and emerge through both bedrock and alluvium near river level (Fig. 5b). A network of much smaller spring vents on both sides of the river reflects the complex karst fracture system but the focus of this study was on the highest discharge springs on the east and west banks. Springs downriver from the Fence fault that were compared hydrochemically to the Fence fault springs include Vasey's Paradise, Travertine Cone Spring, and Hanging Gardens, which all discharge from the R-M aquifer within the downthrown blocks of the Eminence graben.

Fig. 5 a Fence East spring bubbles up, artesian, into the Colorado River. b Fence West emerges from alluvium near river level and gets inundated by the river more easily than Fence East. c-e Vasey's Paradise has variable discharge: c May 17, 2019 has relatively high flow from two cave openings; d May 17, 2013, left vent had lower flow and slightly lighter stable isotope values; e May 19, 2018, both vents were nearly dry

Methods

Water sampling

Water sampling was carried out following procedures set out in the US Geological Survey's National Field Manual for the Collection of Water-Quality Data (USGS 2006). Water samples for cations were collected in 60-ml high-density polyethylene bottles (HDPE). Samples were filtered (0.45 μ m) and acidified using concentrated HNO₃. Samples for anions, alkalinity and δ^{18} O and δ D isotope analysis were collected without headspace in 120-ml HDPE bottles.

Analytical methods

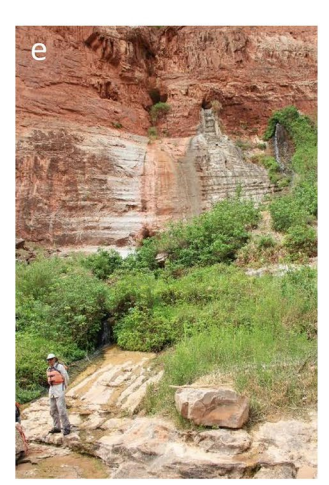
Water temperature, pH, and specific conductance were measured using an Oakton pH/CON 300 multimeter. Major ion chemistry was analyzed using inductively coupled plasma optical emission spectroscopy (cations) and ion chromatography (anions) using standard methods, comparable to US EPA 200.7 and EPA 300.0, respectively. Carbonate alkalinity was measured by titration using standard methods comparable to 2320 ALKALINITY (Baird and Bridgewater 2017). These analyses were carried out at the Analytical Geochemistry Laboratory













at the University of New Mexico (UNM). Isotopologues of oxygen and hydrogen were measured using cavity ring-down spectroscopy (Picarro L1102-I) with methods comparable to Wassenaar et al. (2012) at the Center for Stable Isotopes, UNM. Typical error bars for analyses are $\leq 0.2\%$ for $\delta^{18}O$ and $\leq 0.4\%$ for δD . Total dissolved inorganic carbon (DIC) was calculated using the speciation model PHREEQC (Parkhurst 1995) that uses pH, temperature, and measured alkalinity to estimate all components of the DIC (bicarbonate, carbonic acid, and carbonate).

Continuous monitoring

Unvented multiparameter sensors were deployed for up to 7 years and were downloaded or replaced annually. The parameters monitored were pressure (a proxy for depth), temperature, and specific conductance. The sensors used were Solinst Levelogger Junior Model 3001 LTC. The sensor utilizes piezoresistive silicon with Hastelloy pressure sensor, platinum resistive temperature detector and 4-electrode platinum conductivity sensor. Calibration is not required for temperature and pressure as these come with lifetime factory calibration and are accurate to within 0.1 °C and 0.1% FS (0.5 cm). Calibration is required for conductivity and a 3-point calibration was carried out using conductivity solutions of 1,314, 5,000 and 12,880 µS/cm. For barometric corrections, a Solinst Barologger was used to record air temperature and atmospheric pressure; these were placed in shaded protected areas within tens of meters of the water sensors and were downloaded or replaced at the same times.

Fence East and Fence West springs were monitored. Resolution was initially set at 30-min intervals and reduced to 60 min after the first year. Sensors were deployed within each spring below river level, although the Fence West sensor became partly exposed at lowest flows of ~5,000 cfs (141 m³/s). Data were downloaded in the field using a laptop and infra-red sensor USB connector, and saved as a CSV file. Corrections were made to delete anomalous readings caused by sensors being removed for recalibration/download and anthropogenic

interference, and to make depth corrections for barometric pressure and elevation. Management of continuous monitoring water data was carried out using Excel, Aquarius Time Series software, and MATLAB. Data from a nearby USGS river gauge that continuously measured stage, temperature, and specific conductance in the Colorado River about 1 km upstream of Fence East Spring were also incorporated —Grand Canyon Monitoring and Research Center (GCMRC) and USGS (2021).

Geochemistry

Results

Sample locations, field parameters, stable isotopes and water chemistry are listed in Tables S1 and S2 of the electronic supplementary material (ESM), and mean chemistry data in Table 1. Geochemical results are presented for nine locations: Fence East Spring, Fence West Spring, Fence West Lower (Huntoon's 1981, Diagonal Spring), Vasey's Paradise, Travertine Cone and Hanging Garden springs, Roaring Springs and Bright Angel Creek coming off the south side of the Kaibab uplift, and the Colorado River. Our data closely match older reported field and geochemical parameters for the Fence Springs. Water temperature is ~20 °C, specific conductivity ~2,000 μS/cm. ³He/⁴He ratios in Fence East from previous work had an air-corrected value of ~0.1 R_A, indicating a small but significant proportion (~1%) of mantle-derived helium (Crossey et al. 2006, 2016). Discharge was estimated by Huntoon (1981) as 15.5 cfs (15.5 m³/s) for Fence East Spring and 3 cfs (0.1 m³/s) for the highest discharge spring on the west bank (his Diagonal Spring, but this value is used here for Fence West Spring). Although these discharge estimates were not verified, a ~8-fold higher discharge for Fence East seems reasonable given its stronger artesian character. Other spring vents likely are present below river level making discharge estimates approximate. With the exception of discharge, there is little variation in field parameters or hydrochemistry between Fence East and Fence West springs.

Table 1 Mean chemistry data for springs, in ppm and ‰. n.r. not reported

Spring	Ca ²⁺ (ppm)	Mg ²⁺ (ppm)	Na ⁺ (ppm)	K ⁺ (ppm)	HCO ₃ ⁻ (ppm)	Cl ⁻ (ppm)	SO ₄ ²⁻ (ppm)	δ ¹⁸ O (‰)	δD (‰)
Fence East	176	48	219	21	530	356	249	-14.1	-101.7
Fence West	138	41	174	17	488	257	176	-14.2	-101.4
Fence West Lower	31	20	2	1	197	4	12	-14.0	-100.2
CR-RM-34 (USGS)	60	19	54	3	168	37	167	-14.9	-114.9
Vasey's	47	20	2	1	231	2	5	-13.8	-96.9
Hanging No. 1 ^a	49	19	1	1	217	2	18	nr	nr
Travertine Cone	67	51	30	11	241	30	210	-13.9	-97.4

^aData from Huntoon (1981)



Figure 6a plots temperature (measured in the field) versus total dissolved inorganic carbon (DIC; computed using PHREEQC) and indicates two groups of spring waters. Firstly, Fence East and Fence West springs show relatively

consistent and overlapping values. In field parameters, Fence East mean field temperature = 20 ± 0.3 °C, pH = 6.7 ± 0.3 , and specific conductance = $2,157 \pm 267$ µS/cm; Fence West mean values are: temperature = 21.1 ± 0.3 °C, pH = 6.7 ± 0.3 ,

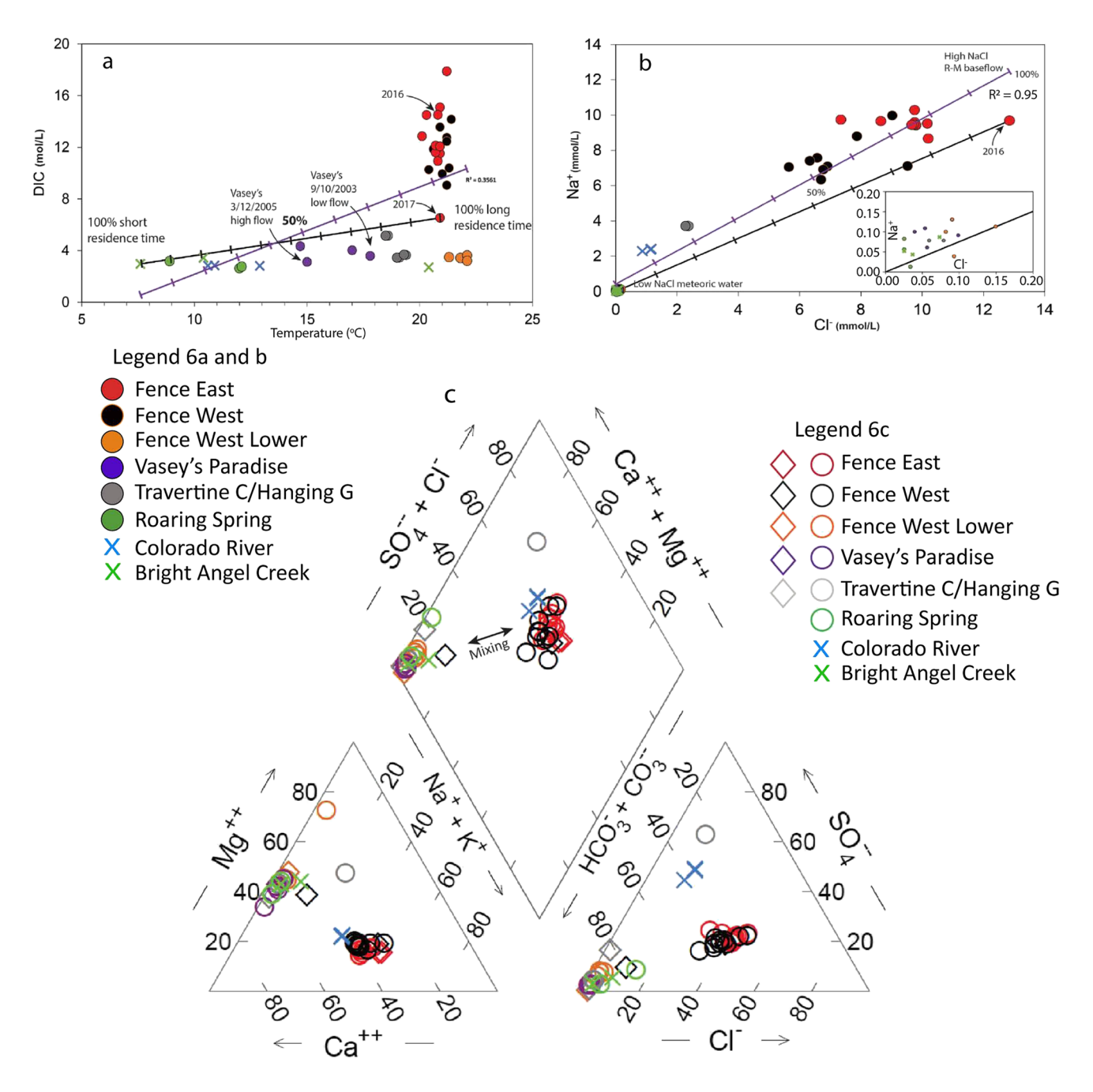


Fig. 6 a Field temperature versus dissolved inorganic carbon (DIC), showing two distinct groups: Fence East and West springs represent karst base flow in the R-M aquifer; graph shows two linear least squares regression lines and mixing proportions based on all data (purple) and selected potential end members (black). **b** Na and Cl content: low NaCl waters in the lower left corner (see inset) includes more meteoric springs; high NaCl waters are from Fence East and Fence West springs. Mixing lines are shown relative to regressed data (purple) and selected potential end member samples (black). **c** Piper

diagram of major element analyses of springs sampled from 1981 to 2019. Two distinct geochemical groups are evident in the parallelogram: Fence East (red) and Fence West (black) overlap suggesting connectivity; near-meteoric springs are seen in Fence West Lower (orange), Vasey's Paradise (purple), Roaring Springs (green circles) and Bright Angel Creek (bright X). The Colorado River (blue X) is hydrochemically distinct from the springs. Open circles are data from this report; open diamonds are from Huntoon (1981). Date format mm/dd/yyyy



and specific conductance = $1,796 \pm 255 \mu S$ over about 17 years of campaign sampling (Table S1 of the ESM). DIC for all the springs ranges from 2.63 to 17.88 mol/L with a mean value of 7.78 mol/L, reflecting the carbonic nature of these springs. Crossey et al. (2009) reported that the DIC for Fence East was derived 45% from the dissolution of limestone in the aquifer, 29% from organic sources (soil gas), and 27% from endogenic (deeply derived/ magmatic sources). Secondly, the other springs, Fence West Lower, Vasey's Paradise, Hanging Garden, and Travertine Cone, are generally cooler, have higher pH, and lower specific conductance (Table S1 of the ESM). Figure 6a shows that they are spread out in temperature (~15-21 °C) at low DIC of 2.5-5 mol/L. The DIC values are more similar to Roaring Springs and Bright Angel Creek, which reflect a larger meteoric component. A plot of Na vs Cl (Fig. 6b) also distinguishes two main water groups with intermediate values, suggesting mixing. Fence East and Fence West overlap, but Fence West has lower salinity; the other springs have very low salinity but the inset shows some spread along the mixing line.

Figure 6c is a Piper diagram (Piper 1944) that shows major cations and anions projected into a central parallelogram; it defines the same two hydrochemical groupings. Water is Na+Ca-HCO₃-dominated, compatible with the carbonic karst nature of these waters with concentrations higher in all ions at Fence East and Fence West springs.

Fence East and Fence West both show a small range of values and are indistinguishable from each other in their major ions. The other group of waters plot close to the left corner of the parallelogram which Crossey et al. (2006, their Fig. 2) interpreted to be close to a meteoric end member; these plot similarly to Roaring Springs and Bright Angel Creek which drain south off the Kaibab uplift. Fence West Lower, Vasey's Paradise, Travertine Cone, and Hanging Garden springs plot closer to the meteoric end member but are displaced slightly towards the Fence springs.

Temporal variation in field parameters and major ion chemistry for karst springs was minimal between the sampling of Huntoon (1981); open diamonds Fig 6c), compared to the 2002 to 2012 sampling reported in this study (Fig. 6). In our sampling, there is least variation in the high discharge Fence East Spring, but, for example, the variation in discharge seen in Vasey's Paradise Spring (Fig. 5c–e) is reflected by different chemistries. Most notably, in 2016, the conservative tracer Cl (9.8 ppm) is several times its values from other years (1.4–2.0 ppm) and is also ~100 ppm higher that year in Fence East and Fence West (454 and 337 ppm, respectively) relative to their mean values of 347 and 257 ppm (Table S2 of the ESM).

Stable isotopes of $\delta^{18}O$ and δD for all Grand Canyon springs resolve into two groups (inset to Fig. 7). Samples plot generally along the Global Meteoric Water Line (GMWL);

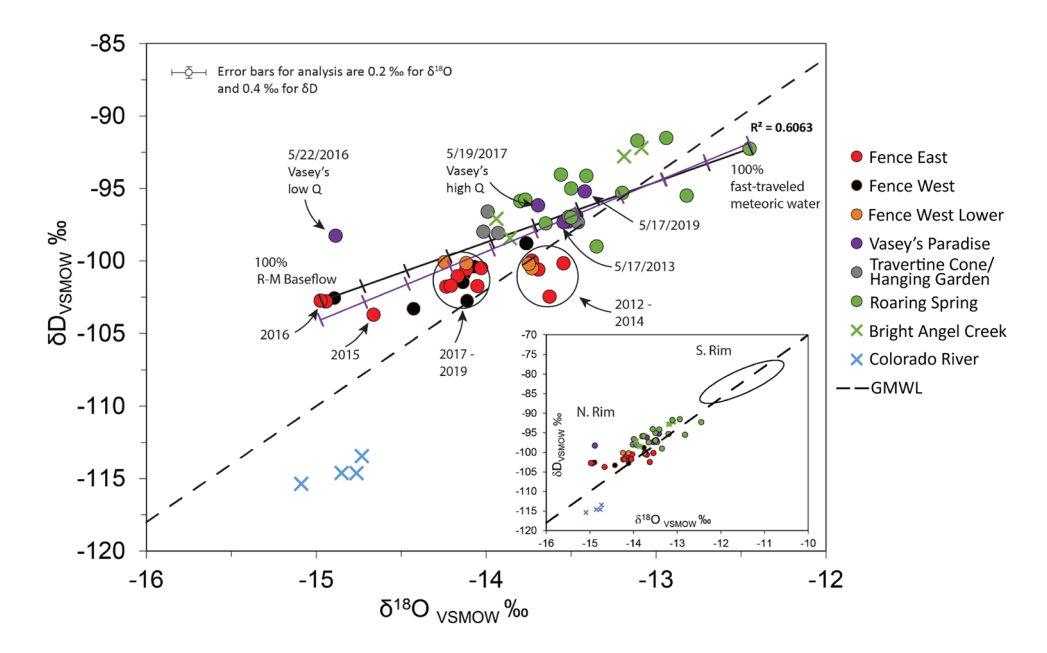


Fig. 7 Stable isotope data for springs in eastern Grand Canyon. GMWL is the Global Meteoric Water Line (Craig 1961). Inset shows regional distinction between North Rim and South Rim waters; South Rim oval drawn from Solder and Beisner (2020, their Fig. 3). Fence East (FE) and Fence West (FW) springs have overlapping values and are distinct from Vasey's Paradise (VP), springs further downstream (FWL, TC, and HG), Roaring Springs (RS) and Bright Angel Creek (BAC), and the Colorado River (CR). Mixing is best documented at

Vasey's Paradise where values are similar to Fence Springs at low flow (larger karst base flow contribution) and similar to Roaring Springs/ Bright Angel Creek at high flow (larger fast flow contribution). Travertine Cone plots along this mixing trend. These data suggest that water from the Fence Springs system is derived dominantly from the Kaibab uplift. Scaled mixing lines are shown relative to linear least squares regression of all the data (purple) and selected potential end-member samples (black).



the inset shows that North Rim-derived groundwater is more negative than South Rim water due to the higher elevation of recharge (Ingraham et al. 2001) and differences in the type of recharge (snowmelt vs monsoonal; Solder and Beisner 2020), and both are distinct from the Colorado River. The Fence Springs system is more depleted in δ^{18} O and δ D than waters derived from the Kaibab uplift such as Roaring Springs and Bright Angel Creek. Fence Springs values for δ^{18} O and δ D range from 13.48 to -14.98% and -96.84 to -103.72%. respectively. Fence East and Fence West springs have δ^{18} O values from -15 to -13.5% and δD values from -100 to −105‰, whereas the more meteoric-dominated springs have generally less negative δ^{18} O of -13 to -15% and $\delta D \sim -92$ to -97%. Temporal variations are noticeable: 2016 δ^{18} O values are more negative in Fence East (two samples), Fence West, and Vasey's Paradise (no sample for Fence West Lower). Potential mixing is suggested by the intermediate locations for Fence West Lower, Travertine Cone, and Hanging Gardens between the more strongly meteoric values of Roaring Springs and Bright Angel Creek and the more negative values at Fence East and Fence West springs.

Figure 8 plots log [1/Cl] versus δD. This plot shows a slight separation between the Fence East and Fence West springs, with Fence East having higher [Cl] (lower 1/[Cl]) than Fence West, although they generally overlap. This slight separation in 1/[Cl] suggests some dilution in Fence West by a meteoric component, as is also seen for the other

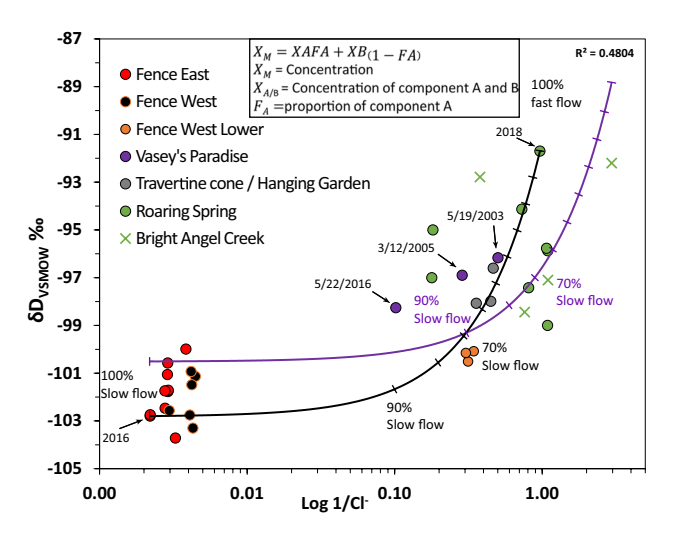


Fig. 8 δD vs 1/[C1]. Clustering of Fence East (FE, red) and Fence West (FW, black) shows similar source and are considered to reflect the karst base flow end member. Fence West Lower (FWL- orange) has similar isotope values, but lower [C1] (high 1/[C1]) similar to Vasey's Paradise. This suggests greater contribution from a fast-traveled end member with some contribution from base flow. Vasey's Paradise variation year-to-year shows a mixing line between the base flow end member (e.g. in 2016 sample) and the fast traveled end member (at high discharge). Curved mixing lines reflects log values on X axis: black = selected end members; purple=regression of all data

springs west of the river. The more meteoric springs spread out considerably suggesting different degrees of mixing.

Interpretation of Geochemistry

Multiple tracers indicate two hydrochemical groups of springs (Figs. 6, 7, 8). Fence East and Fence West springs are interpreted to reflect a near-end member for base flow within the karst aquifer. Springs located off the fault are interpreted to be a mixture consisting of meteoric/fast-traveled water and slow-traveled base flow. Figure 9 shows this interpretation in a schematic cross section that revises the model of Huntoon (1981) to show that groundwater flows west to east from recharge derived from the Kaibab uplift, with no evidence for waters derived from east of Marble Canyon. The greater discharge and artesian character of Fence East spring may be a consequence of subsurface karst plumbing (i.e. derived from flowpaths deeper in the aquifer) rather than different sources with different heads as modeled by Huntoon (1981).

Temperature at the spring vent is a proxy for residence time in the aquifer as meteoric recharge heats to rock temperature. Solute types and concentrations are proxies for the duration of water–rock interaction and rock type. Stable isotopes are a proxy for the source of water molecules themselves (the recharge). All of these parameters are conservative tracers with respect to mixing of waters.

Fence East and Fence West springs show a steady temperature of ~20 °C (Fig. 6a) that has been interpreted to reflect equilibration of karst base flow with rock temperature at the stratigraphic depth of about 800 m (Fig. 2) for a geothermal gradient of 25 °C/km. Other springs show more variation in temperature at lower DIC and mixing lines (Fig. 6a,b) suggests the variation in these waters (14–22 °C) could reflect mixing of up to about 50% karst base flow with fast-traveled waters within different springs and at different sampling times.

The Fence East and Fence West springs have markedly higher Cl and SO₄ ion concentrations that are also interpreted to be characteristic of a deep karst slow-flow end member with appreciable water-rock interaction that has exhibited steady values for decades (Fig. 6c). Mixing lines in Fig. 6b suggests more mixing of meteoric water (up to 50%) in Fence West than in Fence East spring. In contrast, as evidenced by the dye tracer test, fast flow of meteoritic waters from the Kaibab Plateau surface to springs can be on the order of months (Jones et al. 2018). The solute load of Vasey's Paradise, Fence West Lower, Travertine Cone, and Hanging Gardens springs is low, suggesting that these springs are dominated by faster flowpath meteoric waters with an end member best approximated by Roaring Springs and Bright Angel Creek. Mixing of the karst base flow with fast-traveled waters is suggested by the spread in values within Fence Springs and for Travertine Cone (Fig. 6b)



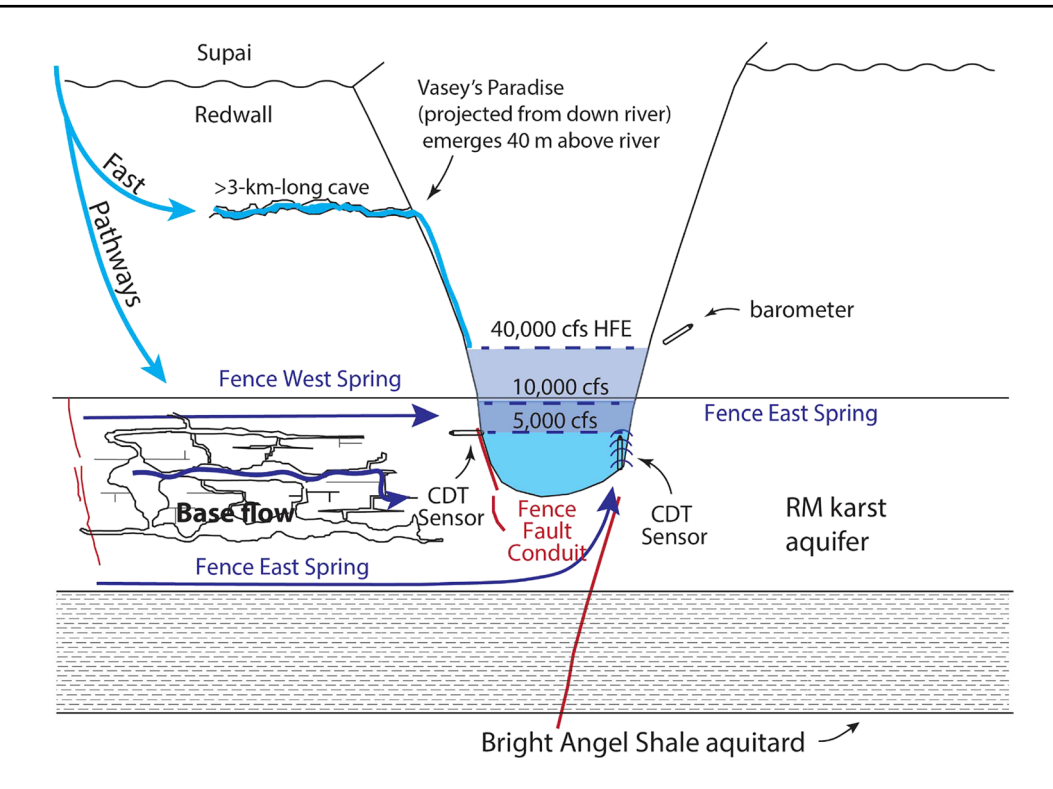


Fig. 9 Schematic of the inferred fast and slow recharge pathways from the Kaibab uplift to springs, and the position of probes. Fence West probe is near the level of the Colorado River at ~10,000 cfs stage; Fence East spring is a bubbling spring that vents into the Colorado River and has an artesian head that displaces river water such that the probe does not feel river temperatures at the level of the probe (~1 m below 10,000 cfs levels) except at high river stages when the river

pressure overcomes the artesian pressure. Vasey's Paradise Spring is projected into this cross section from downriver; it emerges from the Redwall 40 m above the river and shows fluctuating flows related to variable input from fast pathways. The $\sim 40,000$ cfs high flow experiments (HFEs) were dam releases that acted as slug tests to determine aquifer characteristics (see text). 1 cfs = $0.23 \, \text{m}^3/\text{s}$

Isotope values of δ^{18} O and δ D (Fig. 7) also support the conclusion that both Fence East and West springs are similar to each other, but are spread out between end members approximated by karst base flow (Fence East Springs) and predominantly meteoric recharge (Roaring Springs). Roaring Springs itself shows significant variation and its end member (-12.45, -92.26) is used which is similar to the average snowmelt runoff end member (-12.4, -90) identified by Brown (2011). Fence East and West δ^{18} O values are some of the most negative values in the spectrum of Grand Canyon waters and an end member value of (-14.98, -102.74) is used. Given that more negative values are associated with colder, higher elevation recharge (Sharp 2007; Solder et al. 2020), it is inferred that both springs were sourced from Kaibab uplift winter precipitation, and that groundwater flow is from the west to east, opposite to Huntoon's (1981) model. Linear regressions (Faure 2015, pp. 347–348) of all data (purple) and selected extreme values (black; using Roaring Springs) suggest that either end member (karst baseflow and meteoric fast flow) gets mixed with up to ~60% of the other end member at different springs and sampling dates.

The combined tracers (temperature, solutes, and stable isotopes) indicate variable mixing of two distinct water compositions. The karst base flow end member (Fence East and West) salt variation is attributable to up to ~50% mixture (in Fence West) with a very low-salt meteoric end member (Fig. 6b). Variation in the stable isotope composition of the base flow is also attributable to up to ~50% dilution by mixing with a meteoric/fast-traveled end member characterized by Roaring Springs (Fig. 7). This mixing apparently takes place early during recharge as base flow temperature and conductance are steady (Fig. 6a), reflecting long residence time at depth in the karst aquifer. The δD versus log 1/Cl plot shows the bimodality of the two waters in terms of their solutes as also seen in Fig. 6b,c. This log plot emphasizes that the variation in solutes measured in the base flow at Fence Springs is relatively small, with just 10s of % mixture with fast-traveled water reflected by the δD variation. In contrast, springs that are strongly influenced by fast-traveled/ meteoric end member such as Fence West Lower, Travertine Cone, and Vasey's Paradise show ~30, ~40, and up to 60% dilution of karst base flow by the fast-traveled end member,



respectively. Importantly, stable isotopes (Fig. 7) seem to rule out the Colorado River as an important mixing component in the Fence Springs system.

Temporal variations in each of these datasets are considered to be related to changes in spring discharge. This, in turn, is related to the relative proportion of each mixing component, the most variable/changeable being fast-traveled meteoric water—for example, offset of Vasey's Paradise to lighter $\delta^{18}O$ and higher [Cl] is expected at low-discharge times, when karst base flow dominates over faster-traveled meteoric components.

These data are consistent with dye tracer studies (Jones et al. 2018) in that the observed fast response time of meteoric recharge events (especially monsoon storms) seen in some R-M aquifer springs documents the potential for mixing of different end member waters and pathways to produce a wide range of spring compositions. The dye tracer study also documents a direct fast connection (days to months)

between snowmelt recharge and discharge for a portion of the water at Vasey's Paradise (Jones et al. 2018).

Continuous monitoring

Results of Continuous Monitoring

Continuous monitoring results for the Fence Springs system are presented in two parts: description of the 7 years of data for Fence East and Fence West springs (this section) and a detailed look at the spring response to the high-flow experiments (HFEs; see section "Results from the high-flow experiments". Figure 10 schematically illustrates the placement of our probes in the Fence East and Fence West springs in the context of the groundwater flowpath model inferred from the hydrochemistry section of the report, and the varying damcontrolled river stages. During the HFEs, both Fence East

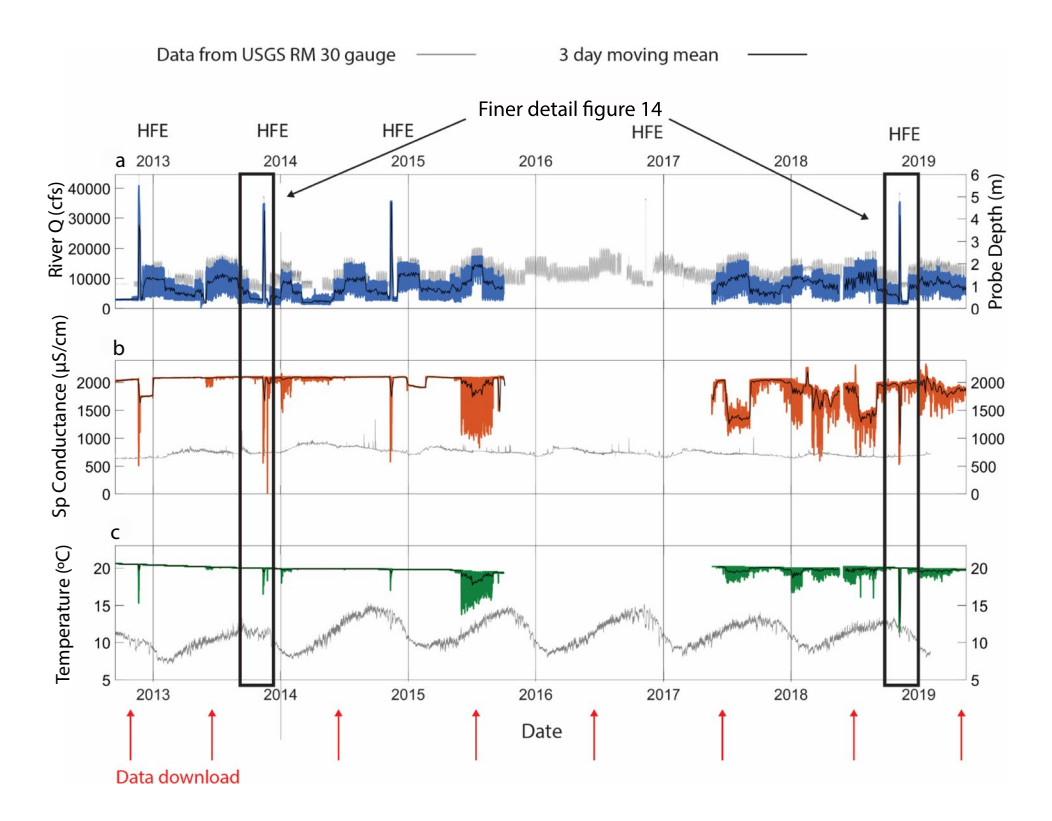


Fig. 10 Fence East Spring continuous sensor data from 2012–2019. **a** Pressure sensor (blue line; depth scale on right axis) is a direct response to river stage (gray curve; cfs on left axis) as measured at the USGS gauge about one river mile upstream. River stage fluctuations occur at daily and weekly cycles depending on electricity demand and dam operations; four high-flows experiments (HFEs) were recorded. **b** Conductance record (orange line) shows trend of progressive decrease of ~100 uS over the 7-year record; river conductance (gray) is from the USGS probe; HFEs caused sharp decreases in conductance due to river water dominance at the level of the probe; note increase in short wavelength conductance variations in 2017–2019 that may reflect

decrease spring discharge. **c** Temperature record (green line) shows steady maximum temperatures and an overall decrease in base flow maximum temperature of ~1 °C over 7 years; early years are characterized by very stable values. River temperature at the USGS probe (gray) shows seasonal variation not seen in the spring. HFEs cause short-term dramatic decrease in recorded temperature reflecting river water pushing down on and overwhelming the artesian spring. Note that increase in short-wavelength temperature variations in 2017–2019 may reflect decreased spring discharge. The time of downloads is shown by red arrows; in general, these do not correspond to major changes in the time series. Black lines are the 3-day running means. 1 cfs = $0.23 \text{ m}^3/\text{s}$



and West springs were inundated by several meters of river water for periods of several days which pushed river water down into spring vents and the karst aquifer, acting like a slug test. The recovery response of each of the Fence Springs to the individual HFEs varied due to the magnitude, total duration, and length of peak discharge of each HFE, as well as river stage prior to the HFE.

Fence East erupts upwards with considerable artesian force at the edge of, and directly into, the Colorado River (Fig. 5a). Its probe was submerged at all times within the upward bubbling spring about 1 m below the surface. Fence West is near the end of a sand bank (Fig. 1c) and forms a relatively calm pool at river level (Fig. 5b) and the probe becomes partly emergent at low river stages. Fence East has a higher discharge of 15.5 cfs (410 m³/s) compared to Fence West 3 cfs (0.1 m³/s; Huntoon 1981).

Figures 10 and 11 show full data streams, by parameter, for Fence East and Fence West. Descriptive statistics about each HFE are in Table 3. Gaps in the record are due to either failure of the sensor, years for which park permits could not be obtained, and/or there was limited memory for new readings. Some variations in the data may be due to slight

differences in sensor position but times of data downloads (red arrows in Figs. 10 and 11) in general do not correspond to changes in the time series arguing that the data record real variations at the probe due to spring—river interactions and long-term trends. Both springs were shielded from the full impact of the change in river stage and velocity, being close to the canyon walls, and the authors argue that because major trends can be seen in both springs, they do not significantly reflect deployment variables.

Interpretation of 7 years of Continuous Monitoring

Measured depth values (right-hand Y-axis, Figs. 10 and 11) record variations in the depth (in meters) from the location of the sensor to the water surface. The depth of the sensor co-varies with river discharge (left-hand Y axis, gray curve) that varies between 5,000 and 20,000 cfs (141–566 m³/s) due to controlled releases from Glen Canyon Dam, with much higher variation during the high-flow experiments (HFEs). Because the sensors were deployed mainly below river level, the dominant signal in the depth data is the variation in river

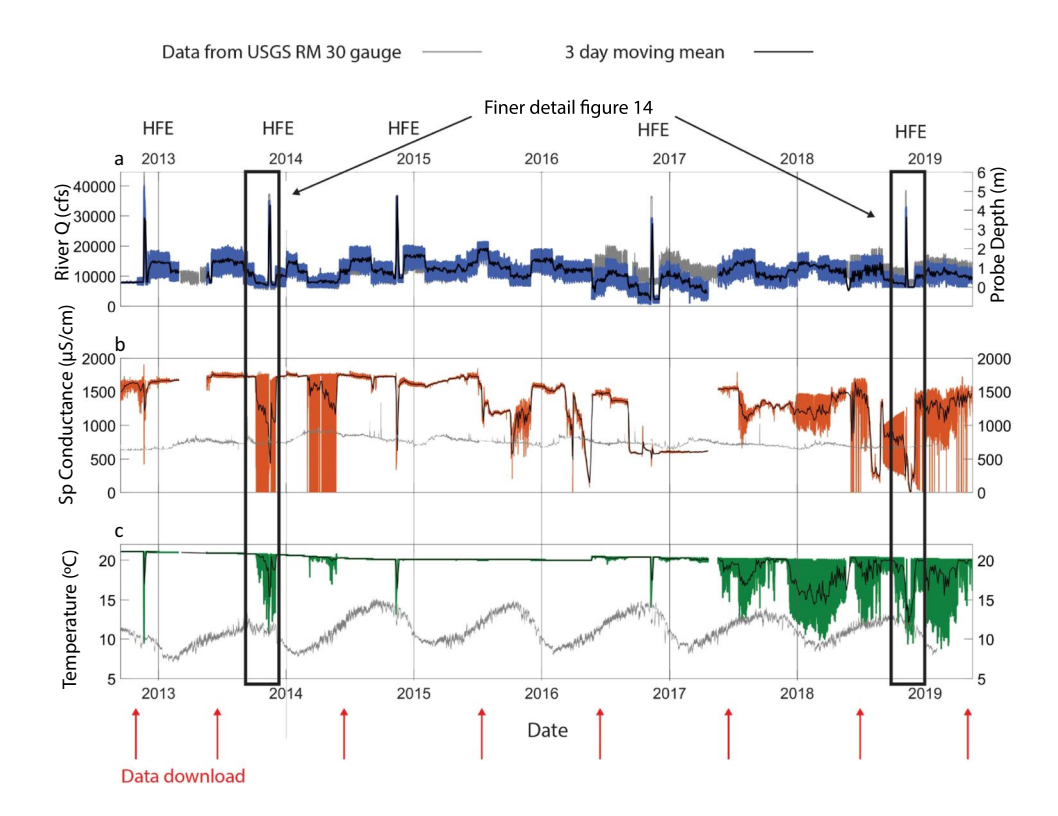


Fig. 11 Fence West Spring continuous sensor data from 2012–2019. **a** Pressure sensor (blue line; depth on right axis) is a direct response to river stage (gray curve; cfs on left axis) as measured at the USGS gauge about one river mile upstream, including during five HFEs. **b** Conductance record (orange line) shows overall trend of decrease of ~100 μS; HFEs caused sharp decreases in conductance due to river water dominance. **c** Temperature record (green line) shows an overall decrease in

base temperature of ~1 °C over 7 years, with periods of most stable values in 2012–2013 and 2015–2017. HFEs caused dramatic decrease in recorded temperature reflecting river water inundation. Increase in short wavelength temperature variations in conductance and temperature after 2017 could reflect decrease in discharge. Gray lines (b-c) are values from the nearby USGS gauge on the Colorado River. 1 cfs = 0.23 m³/s



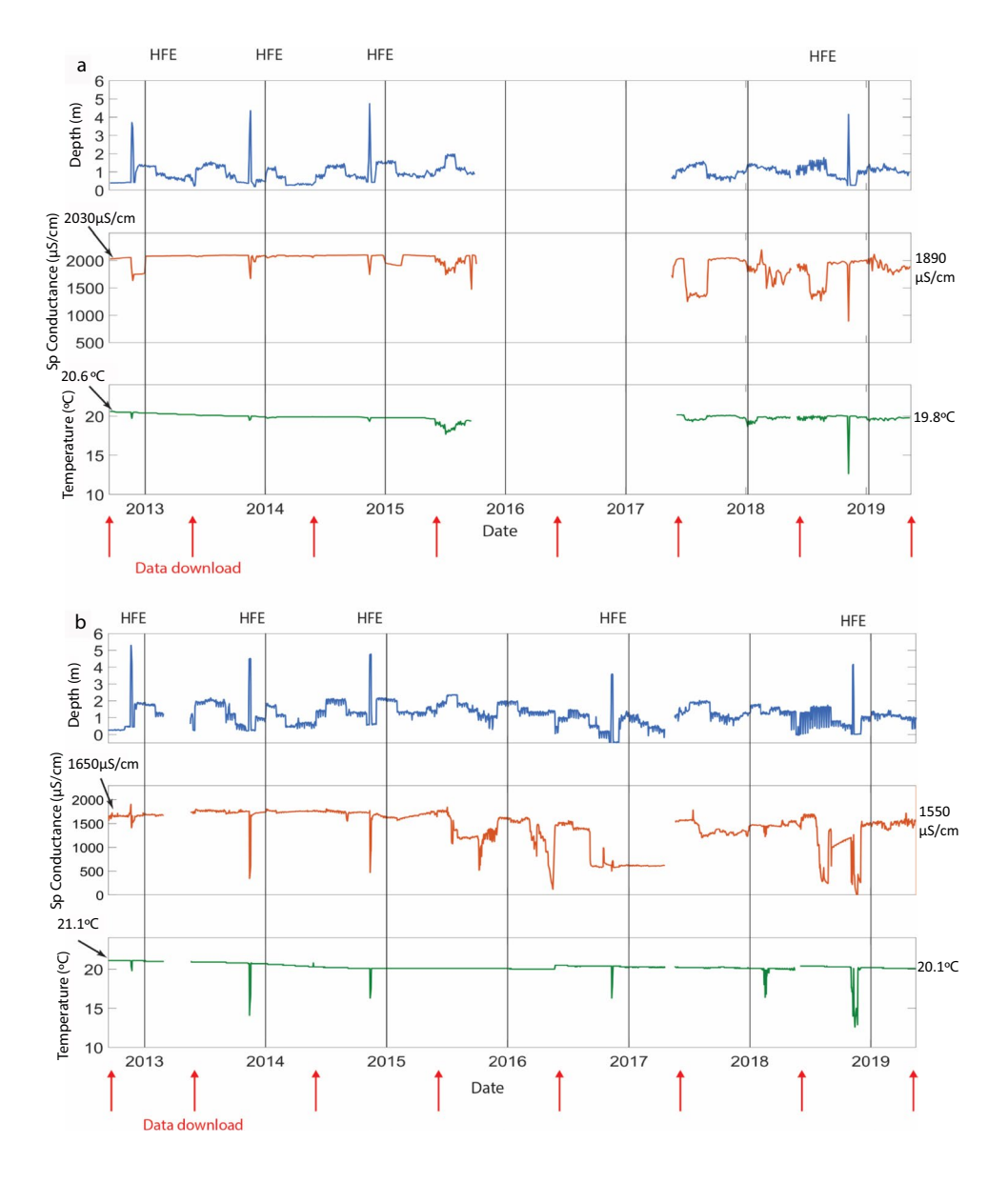
level, even for the Fence East Spring, which remains artesian and does not mix with river water until high river stages.

Baseflow temperature in both Fence East and West springs has been relatively unchanging, especially in the 2012–2013 timeframe, indicating that the spring's discharge is unaffected by seasonal snowmelt or punctuated monsoonal events such as are seen at nearby Vasey's Paradise and Roaring Springs (Jones et al. 2018). This suggests high storage capacity in the karst aquifer and slow fracture flow. The ~20 °C temperature is interpreted to reflect thermal water–rock equilibration at ~800 m depth at a geothermal gradient of about 25 °C/km. We envision a large storage region in the lowest portion of the Eminence graben that houses a significant reservoir of slow-moving water in the R-M karst system. However, over the 7-year timespan, the maximum value of temperature has progressively decreased

by ~1 °C in both springs. This reinforces the interpretations of the hydrochemistry section of the report that the aquifer is connected beneath the river (Fig. 9) and that these springs can be considered as an end member representative of the karst baseflow for the Marble Canyon region.

Maximum value of specific conductance has a similar signal to temperature. Figure 12 shows our interpretation that the long-term decrease in temperature of ~1 °C in both springs was accompanied by a decrease in specific conductance of $100-140~\mu S/cm$ over the recording period. Both changes can be explained in terms of a decrease in the discharge of the R-M base flow if it is accompanied by an increasing proportion of fast-traveled meteoric components in this part of the R-M aquifer. This period of time (2012-2019) has been a time of declining meteoric recharge on the Kaibab uplift, measured in terms of decreasing mean yearly snow water

Fig. 12 a Fence East and b
Fence West daily maximum
values are considered to be closest to spring values and most
representative of the karst base
flow component. Long-term
decrease in both specific conductance and temperature across
the 7-year period is interpreted
to reflect decreased discharge of
both springs





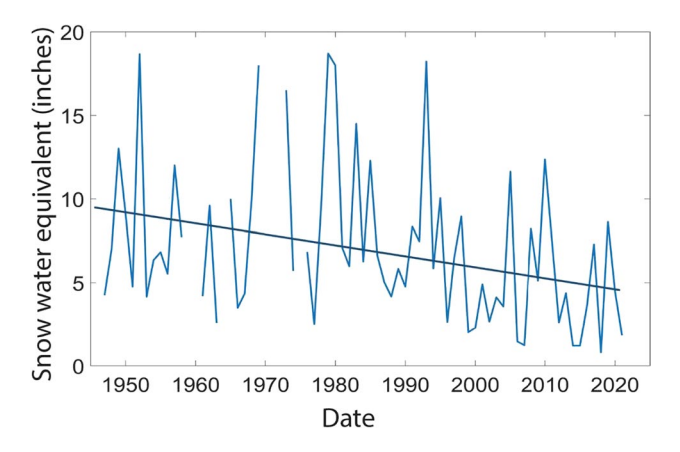


Fig. 13 Snow-water equivalent mean yearly values from the Bright Angel Station, North Rim, Grand Canyon (Natural Resources Conservation Service, NRCS, and USDA 2021); regression line shows a decrease in snowpack across the record period and a likely decrease in fast-travelled, meteoric recharge to the karst aquifer. 1 inch = 2.54 cm

equivalent (Fig. 13). Thus, our interpretation is that reduced discharge reflects both reduced meteoric recharge volume and an even more reduced R-M karst baseflow. Decrease in the overall karst baseflow is also supported by the greater fluctuation in temperature and specific conductance seen after 2015 in Fence East spring.

Alternatively, the observed 7-year decrease in temperature and specific conductance could reflect a very old age for the baseflow waters that may have been recharged during a cooling period much earlier, in the 1900s or even in cooler climate regimes farther in the past-for example, winter snowpack may have been greater several decades ago than now, and early Holocene climates were cooler and wetter (Woodhouse et al. 2010). The implication of this hypothesis of older recharge would have less immediate societal implications for the karst base flow. However, the subtle variation in geochemistry seen in stable isotopes among the Fence subsidiary springs, the temporal variation and indication of mixing trends in Vasey's Paradise and other downstream springs, and the increased fluctuation of temperature and conductance in both springs in 2013-2014 compared to 2016–2019, during a time of warmest summer temperatures, decreased Bright Angel Creek base flow, and lowering snowpack, lead us to favor the hypothesis of decreasing baseflow at the one-decade timescale.

Results from the High-Flow Experiments

Our sensors were in place during five high-flow experiments (HFEs; Fig. 14) that were conducted by the Bureau of Reclamation as a part of the management of the Glen Canyon Dam (Melis 2011). A USGS probe in the Colorado River located ~1 km upstream also recorded river stage (height

of river surface) and calculated discharge, temperature, and conductivity in the Colorado River (gray lines on the depth curves of Fig. 14). Each HFE had a somewhat different hydrograph, but in general, at the location of the installed sensors, the river raised quickly from <1 m (~5,000 cfs, 141 m³/s) to >5 m depth (~40,000 cfs, 283 m³/s) over a short ramp-up time of ~8 h. Peak flows were maintained for several days, then ramped down at a slower rate than the abrupt ramp-up.

Depth data from the spring probes record the spring's response at the several-day timeframe (Fig. 14; Table 2). Prior to the experiments, Colorado River discharge from the dam was held constant at about 5,000 cfs (141 m³/s) for ~7 days. Water was then released from Glen Canyon Dam to the Colorado River by jet tubes with peak discharge being reached in 24 and 96 h. As the pulse of water moved downstream, it spread out depending on channel width. The HFEs arrived at Fence Springs 9–14 h after dam release traveling at ~2–3 MPH (3–5 KPH). When the crest arrived, river depth above the probes increased by 4–5 m (about 35,000–40,000 cfs, 991–1,132 m³/s). This piled water above the springs and pushed river water down past the probes, lowering spring specific conductance and temperature within the spring to near-river values (Table 3).

Specific conductance can also be used as a conservative tracer to estimate mixing proportions between river and groundwater end members. Variations of minimum specific conductance at the probe during the HFEs show a distinction between Fence East and Fence West springs, and between the early and later HFEs in both springs. Fence East specific conductance (Fig. 14) showed earlier response than temperature in 2012, 2013, and 2014 with values approaching river values during the ramp-up stage, several hours before the spring reached its minimum (most river-influenced) temperature. Specific conductance fluctuated wildly between river and spring values throughout the HFE. Recovery at the end of the experiment was slower and, especially in 2012, took several days past the return to post-HFE river stage. In 2018, specific conductance quickly reached its minimum value at the onset of the ramp-up, fluctuated, but maintained near-river values during much of the HFE, and recovered within a day of return to pre-HFE river stages. Thus, there was a partial decoupling of temperature and specific conductance signals.

Fence West specific conductance response took two forms (Fig. 14). There was a 'square' response in years 2013 and 2018 in which specific conductance values are a mirror image of river stage and the spring took on river values throughout the HFE. These are years in which the pre-HFE installation was such that the probe was exposed to the air regularly during the low flows before the HFE, explaining the values of ~500 μ S/cm, well below river values of ~800 μ S/cm. In years 2012 and 2016, Fence West Spring showed a 'sine wave' response



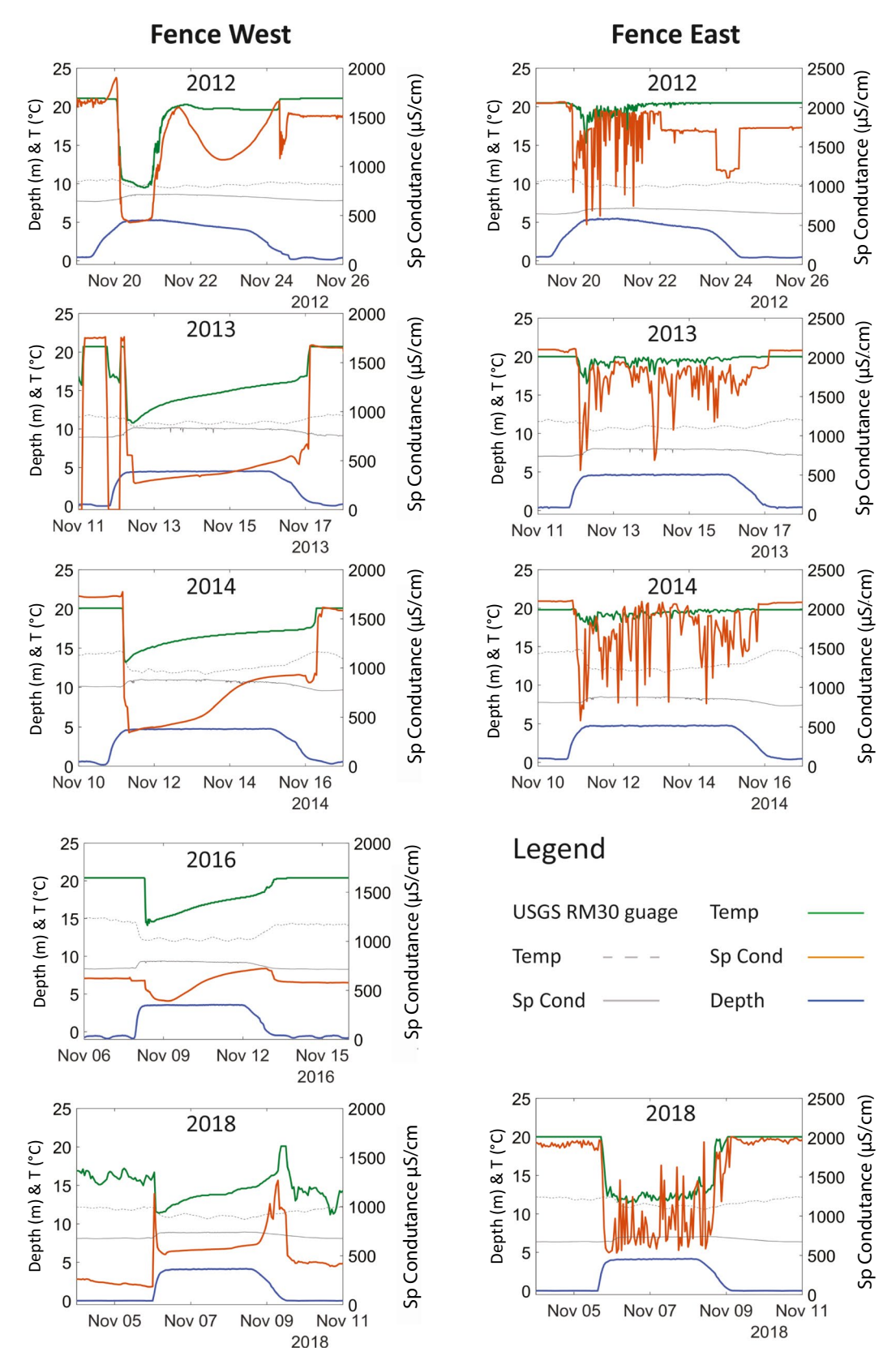


Fig. 14 High-flow experiments: continuous sensor records of specific conductance (orange, right Y-axis), temperature (green; left Y-axis) and depth (blue, left Y-axis) response in Fence Springs from the 2012, 2013, 2014, 2016 (FW only), and 2018 Colorado River HFEs;

analogous to a slug test of the karst aquifer. The upper gray-dashed line shows specific conductance of the river and the lower thin black line shows river temperature, both recorded at the USGS sensor



in which specific conductance lowered by $500-1,500~\mu S/cm$ quickly after the HFE initial ramp-up, mimicking temperature decrease, then recovered to near spring values in the late stages of the high-flow, then decreased after the ramp-down, presumably because of disturbance and emergence of the probe site after ramp-down. The 2014 HFE response has both the square drop and rise coinciding with the ramp-up and ramp-down like 2012 and 2018, but also partial recovery during the HFE like 2014 and 2016.

Temperature is accurately measured by the sensors (to ± 0.1 °C) and provides a sensitive conservative tracer that can be used to evaluate mixing proportions between groundwater and river water at the probes through the time of the HFEs. The temperature variations during the HFEs in Fence East Spring were relatively similar for the early HFEs (2012–2014) but somewhat different in 2018. The minimum temperature recorded at the probe through the time of the HFE records the times of greatest effect of mixing of river and groundwater at the probe (green curves of Fig. 14). In 2012 to 2014 HFEs, at Fence East, cooling by up to 5 °C (e.g. in 2012) occurred quickly (within hours) upon arrival of the HFE pulse. The temperature however recovered about half (2 °C) of that loss in ~12 h and then fluctuated at about ±3 degrees during the HFE, then recovered completely and returned to steady groundwater values at the end of, or during, the ramp down. This threshold at which the spring returned to steady values, when it no longer felt the effect of the HFE, was about 20,000 cfs (566 m³/s) in 2012 and 2013 but only 10,000 (283 m³/s) in 2014. The 2018 HFE has a different temperature response in that it underwent a larger sharp temperature decrease of 8 °C upon arrival of the HFE, then fluctuated (again by 1–2 °C) at this cooler temperature until the beginning of the ramp-down, then recovered at a lower threshold stage of $\sim 9,000 \text{ cfs } (255 \text{ m}^3/\text{s}).$

The Fence West Spring temperature was monitored through all 5 HFEs. With the exception of 2012, the HFEs from Fence West have an asymmetric, skewed shape with a sharp decrease at the onset of the high-flow followed by a steady recovery and return to pre-HFE values coinciding with different points along the ramp-down. Temperatures dropped ~10 °C in the space of 1–2 h, while the return lasted the length of the HFE. The "threshold river stage" when the spring regained pre-HFE values, decreased from 8,000 cfs (226 m³/s) in 2013, 7,500 cfs $(212 \text{ m}^3/\text{s})$ in 2014, 7,000 cfs $(198 \text{ m}^3/\text{s})$ in 2016, to 6,500 cfs (184 m³/s) in 2018. In contrast, the HFE in 2012 has a distinct shape in that the HFE peak discharge was ramped up quickly and achieved the highest discharge of ~43,000 cfs (1,218 m³/s) of all the HFEs (Table 2). Spring temperature dropped quickly (4 h) to near river temperatures of 10–11 °C. Recovery to 20 °C (>90% of the difference between spring and river temperature) took place after only a few hours suggesting a threshold value of ~40,000 cfs (1,132 m³/s) for 90% recovery, but full recovery to 21 °C occurred 2 days later when stage reached ~10,000 cfs (283 m³/s) during ramp down.

Table 2 High flow experiments (HFE) comparison data

Year	Duration	(days, hours)	River discharge (cfs) ^b			
	Total	Peak ^a	Max ^c	Pre/post HFE ^d		
2012	3, 19	24 h	43,000	7,000/9,000		
2013	5, 5	96 h	37,000	7,000/9,000		
2014	5, 5	96 h	37,500	7,000/9,000		
2016	5	9 h	36,500	7,000/9,000		
2018	3, 10	60 h	38,100	6,500/9,000		

^aPeak refers to time of peak river stage after start of experiment

Interpretation of High Flow Experiments

Variations in depth, specific conductance and temperature occurred during high-flow experiments and these fluctuations increased in frequency and amplitude during the high stages of HFEs after ~2015. A close correspondence of oscillations of mean depth with mean river stage is seen in both Fence East and Fence West springs as shown by the comparison to the USGS probe (Figs. 10 and 11). These fluctuations are interpreted to reflect inundation of the springs by river water during high-flow experiments and, for non-HFE times, swaying of the sensor in turbulent upwelling spring water that may mix with some river water.

Specific conductance and temperature in both Fence East and Fence West springs are demonstrably lowered during

Table 3 Spring parameter descriptive statistics

Spring	Discharge Q (cfs)	Specific conductance (μS/cm)			Tem- perature (°C) ^c	
		Max	Min	Mean	Max	
Fence East ^b	15.5	2,540	~500d	1,933	20.6 ^d	
FenceWest ^b	0.1	2,340	~350d	1,310	21.1 ^d	
Fence West Lower ^a	2	378	338	348	22.1	
USGS gauge RM-34	5,428–4,4644	1,337	627	740	15.4	
Vasey's Paradise ^a	5.5	469	268	368.5	19.4	
Hanging Graden ^a	0.07	366	366	366	18.7	
Travertine Cone ^a	0.07	414	346	380	19.4	

^aField values from hand-held instrument

^dExcludes higher/lower values when probe was above river level



 $^{^{}b}cfs$ cubic feet per second (1 cfs ~ 0.0283 m³/s)

^cMax maximum river discharge during the experiment

^dPre/post refers to river discharge before and after the experiment

^bValues from sensor

^ccfs cubic feet per second (1 cfs ~ 0.0283 m³/s)

high river stages of the HFEs (40,000 cfs, 1,133 m³/s) but were unaffected in 2013-2015 by normal dam-controlled river fluctuations of 5,000-15,000 cfs ($141-425 \text{ m}^3/\text{s}$). In contrast, after 2015, the same river fluctuations caused frequent lowering of specific conductance and temperature maximum values at stages below 10,000 cfs (283 m³/s). This may have been caused or amplified by the less stable deployment of the Fence East probe allowing more mixing with river water, but because it is observed in both springs, and in both specific conductance and temperature, this temporal change reinforces the interpretation of decreased karst base flow between 2012 and 2018 such that the springs were more readily infiltrated by river water below a threshold stage of ~10,000 cfs (283 m³/s). The different threshold values are compatible with the decreasing artesian head of the Fence East Spring from 2012 to 2018.

The HFE demonstrated an overall resilience of the R-M aquifer in eastern Grand Canyon. The river high flows caused an essentially instantaneous increase in hydraulic head (at the scale of meters of stage height), then a quick drop back to normal flows. This increase was sufficient to almost stop the artesian flow of the Fence system at the measurement location (based on temperature monitoring). Both springs recovered to pre-HFE temperatures before or within a few hours after ramp down. In 2012–2014, the rapid recovery to warmer groundwater temperatures takes place on a time scale of hours, however the conductance recovery was more complex and indicates the occurrence of isothermal mixing in the aquifer near the spring.

Conclusions

The combination of hydrochemistry and a 7-year record of autonomous sensor monitoring of the Fence Springs system provides unusual resolving power for understanding the karst aquifer system of eastern Grand Canyon. This spring system consists of multiple springs that all emerge from the R-M aquifer near river mile 30 in the Eminence graben of eastern Grand Canyon. The Fence springs characterize the base flow of the Marble Canyon portion of the R-M aquifer and different spring hydrochemistries reveal variable mixing with fast-traveled meteoric recharge. These are both essential elements for understanding and managing the hydrologic resources of the arid Colorado Plateau region.

Geochemistry from campaign sampling suggests that the Fence Springs have maintained similar major ion chemistry since the 1980s. These springs are warmer, higher TDS, higher alkalinity, and isotopically heavier than the Colorado River. The authors support the model of Huntoon (1981) that these springs are connected by a confined karst aquifer system beneath, but do not mix with, the Colorado River. However,

instead of the proposed east–to-west groundwater flow (Huntoon 1981), stable isotopes of $\delta^{18}O$ and δD indicate that water discharging from Fence East and Fence West springs has isotopic values consistent with North Rim recharge, derived from the Kaibab Plateau to the west of the river, and that flow is from west-to-east. Fence Springs show that the base flow for Marble Canyon of eastern Grand Canyon is 20 °C, specific conductance of ~2,000 μ S/cm, and $\delta^{18}O$ of ~ -14%.

Multiple tracers in Vasey's Paradise, Hanging Gardens, and Travertine Cone springs, west of the river, identify a second main hydrochemical component made up of a higher proportion of meteoric/fast traveled water that is cooler, has lower TDS and alkalinity, and heavier isotopic values of $\delta^{18}O = -13\%$ and $\delta D = -94\%$. Roaring Springs on the south side of the Kaibab uplift is taken as representing this more meteoric end member. The significant variation for both end member springs, plus the intermediate composition springs, suggest the mixing of a variable proportion of meteoric/fast-traveled groundwater (similar to Roaring Springs) with karst base flow (similar to Fence Springs). A higher proportion of fast pathway flow produces more variable spring discharge, hydrochemistry, and increased seasonality that indicates they are affected by recharge pulses from both monsoonal and snowmelt events. All the springs of this study emerge from the R-M aguifer such that they offer the potential generalization for karst aquifer springs of Grand Canyon—that their character reflects spatially and temporally complex mixing between waters traveling in the karst base flow and fast-traveled additions.

Seven years of data from autonomous sensors deployed in both Fence East and Fence West springs corroborate the conclusions from hydrochemistry. Both springs show the same steady (relatively invariant) maximum values of temperature and specific conductance for extended periods and the springs are not affected by seasonal variations or pulses from snowmelt or monsoonal precipitation. This reflects a large storage capacity within the aquifer and confirms that the springs are part of a uniform karst base flow for Marble Canyon of eastern Grand Canyon. The higher discharge and greater artesian pressure in Fence East spring is interpreted to reflect a west-to-east flowpath that is slightly deeper in the R-M aquifer that emerges up the Fence fault zone into the base of the Eminence graben.

Perhaps the most impactful observation of our long-term spring monitoring is a monotonically steady decrease by ~1 °C and an accompanying decrease in specific conductance of 100–140 μ S/cm observed in both Fence Springs. These decreases are interpreted to indicate a reduction in discharge from this part of the RM aquifer accompanied by an increased proportion of meteoric/ fast-traveled waters. This has taken place during the warmest, driest recharge years in recorded history, such that it is not likely to be attributed to an increase



in recent meteoric recharge, and instead implies a decrease in karst base flow in this part of the aquifer caused by and accompanying an even greater decline in meteoric recharge. This decadal trend has implications for future continued 'mining' of aquifer waters. If this trend continues, there are risks to human water supply and water quality (water hardness and solute content increases as recharge diminishes), but also to ecosystems and protected species like the humpback chub that relay on the warmer spring water of the Little Colorado River and Fence Springs to provide breeding habitats within the markedly cooler waters of the Colorado River.

The fortuitous deployment of sensors and the response of Fence Springs through five high-flow experiments from 2012-2018 reinforces several of our main conclusions. A decrease in discharge of the karst base flow that feeds the Fence Springs is supported by the change in response between 2012-2013 and 2017-2018, in both springs, but especially at Fence East Spring (the higher discharge spring). The 2017–2018 HFEs of similar stage (~40,000 cfs, 1,132 m³/s) had greater impact on the springs-both temperature and specific conductance were lowered more, were more variable, and were maintained at values closer to river level values, suggesting less groundwater discharge and lowered head. Due to its lower variability and response to the HFE's, and much higher discharge, Fence East Spring may provide the more robust "canary" to warn about changing deep R-M groundwater in springs sourced from the eastern part of the Kaibab uplift and should continue to be monitored.

This effort to combine hydrochemistry and spring monitoring is a start toward developing a water base line for the karst aquifer system in Grand Canyon and the larger Colorado Plateau region. Lessons learned from our monitoring effort are to minimize temporal gaps by more regular data download, establish better-fixed probe installations with known year-to-year stability such that deployment variables and download events that can compromise data quality are minimized. Adding specific conductance to temperature and depth in probes adds an essential dimension (continuous water chemistry) to decipher complex karst systems and water mixing. Establishing probes in more of the major R-M karst springs as well as deep wells at Valle, Tusayan, Canyon Mine, and other well locations, is needed to monitor temporal and spatial variations in the regional karst baseline.

Supplementary Information The online version contains supplementary material available at https://doi.org/10.1007/s10040-022-02541-1.

Acknowledgements We would like to thank Abdul-Medhi Ali, Viorel Atudorei and Laura Berkemper for laboratory assistance (the UNM Analytical Laboratory, and Center for Stable Isotopes respectively). We thank Cameron Reed for help with drafting and Grand Canyon National Park (GRCA) for research and collecting permits throughout the study. Reviews by Daniel Doctor and Don Sweetkind helped improve the report.

Funding We acknowledge NSF grant EAR- 0538304 from the Hydrologic Sciences Program (01/01/2006-12/31/2007) to L. Crossey, K. Karlstrom, T. Fischer, and A. Springer, and student awards to C. McGibbon from Cindy Jaramillo Graduate Scholarship 2019, The Patrick J.F. Gratton Scholarship fund 2018, The Geology Alumni Scholarship fund 2017, GPSA Student Research Grant 2017.

Declarations

Conflict of interest On behalf of all authors, the corresponding author states that there is no conflict of interest.

References

- Baird R, Bridgewater L (2017) 2320 ALKALINITY, Standard methods for the examination of water and wastewater, 23rd edn. American Public Health Association, Washington, DC
- Adams EA (2005) Determining ephemeral spring flow timing with laboratory and field techniques: Applications to Grand Canyon, Arizona. MSc Thesis, Department of Geology, Northern Arizona University, Flagstaff, AZ
- Billingsley GH, Hampton HM (2000) Geologic map of the Grand Canyon 30' x 60' quadrangle, Mohave and Coconino counties, northwestern Arizona. US Geol Surv Miscell Geol Invest Ser I-2688, scale 1:100.000
- Bills DJ, Flynn ME, Monroe SA (2007) Hydrogeology of the Coconino Plateau and adjacent areas, Coconino and Yavapai counties, Arizona. US Geol Surv Sci Invest Rep 2005-5222. https://doi.org/ 10.3133/sir20055222
- Bills DJ, Flynn ME, Monroe SA (2016) Arizona Water Science Center. US Geol Surv Fact Sheet 113-02
- Brown C (2011) Physical, geochemical, and isotopic analyses of R-Aquifer springs, North Rim, Grand Canyon, Arizona. MSc Thesis, Northern Arizona University, Flagstaff, AZ
- Cooley ME, Harshbarger JW, Akers JP, Hardt W, Hicks ON (1969) Regional hydrogeology of the Navajo and Hopi Indian reservations, AZ, NM, UT. US Geol Surv Prof Pap 521-A. https://doi. org/10.3133/PP521A
- Craig H (1961) Isotopic variations in meteoric waters. Science 133:1702-1703
- Crossey LJ, Fischer TP, Patchett PJ, Karlstrom KE, Hilton D, Newell D, Huntoon P, Reynolds A, Leeuw G (2006) Dissected hydrologic system at the Grand Canyon: interaction between deeply derived fluids and plateau aquifer waters in modern springs and travertine. Geology 34:25–28. https://doi.org/10.1130/G22057.1
- Crossey LJ, Karlstrom KE, Springer AE, Newell D, Hilton D, Fischer TP (2009) Degassing of mantle-derived CO2 and He from springs in the southern Colorado Plateau region: neotectonic connections and implications for groundwater systems. Geol Soc Am Bull 121:1034–1053. https://doi.org/10.1130/B26394.1
- Crossey LJ, Karlstrom KE, Schmandt B, Crow R, Colman D, Cron B, Takacs-Vesbach TD, Dahm C, Northup DE, Hilton DR, Ricketts JR, Lowry AR (2016) Continental smokers couple mantle degassing and unique microbiology within continents. Earth Planet Sci Lett 435:22–30. https://doi.org/10.1016/j.epsl.2015.11.039
- Faure G (2015) Isotopes principles and applications. Wiley, New York Grand Canyon Monitoring and Research Center (GCMRC), USGS (2021) Colorado River above Little Colorado River near Desert View, AZ 09383100, sediment and water quality data. www.gcmrc.gov/discharge_qw_sediment/station/GCDAMP/09383 100#. Accessed Sept 2022



- Huntoon PW (1974) The karstic groundwater basins of the Kaibab Plateau, Arizona. Water Resour Res 10:579–590. https://doi.org/ 10.1029/WR010i003p00579
- Huntoon PW (1981) Fault controlled ground-water circulation under the Colorado River, Marble Canyon, Arizona. Ground Water 19:20–27. https://doi.org/10.1111/j.1745-6584.1981.tb03433.x
- Huntoon PW (2000) Variability of karstic permeability between unconfined and confined aquifers, Grand Canyon region, Arizona. Environ Eng Geosci 6:155–170. https://doi.org/10.2113/gseegeosci.6.2.155
- Huntoon PW, Sears JW (1975) Bright Angel and Eminence Faults, Eastern Grand Canyon, Arizona. Geol Soc Am Bull 86:465–472. https://doi.org/10.1130/0016-7606(1975)86<465:BAAEFE>2.0.CO:2
- Ingraham NL, Zukosky K, Kreamer DK (2001) Application of stable isotopes to identify problems in large-scale water transfer in Grand Canyon National Park. Environ Sci Technol 35(7):1299–1302. https://doi.org/10.1021/es0015186
- Jones CJR, Springer AE, Tobin BW, Zappitello SJ, Jones NA (2018) Characterization and hydraulic behaviour of the complex karst of the Kaibab Plateau and Grand Canyon National Park, USA. Geol Soc Spec Publ 466:237–260. https://doi.org/10.1144/SP466.5
- Kessler JA (2002) Grand Canyon Springs and the Redwall-Muav Aquifer: comparison of geologic framework and groundwater flow models. MSc Thesis, Northern Arizona University, Flagstaff, AZ
- Lange AL (1956) Cave evolution in Marble Gorge of the Colorado River. Plateau 29:12–21
- Melis, TS, ed., 2011 Effects of three high-flow experiments on the Colorado River ecosystem downstream from Glen Canyon Dam, Arizona. US Geol Surv Circ 1366, 147 pp
- Metzger DG (1961) Geology in relation to availability of water along the South Rim Grand Canyon National Park Arizona. US Government Printing Office, Washington, DC
- Monroe SA, Antweiler RC, Hart RJ, Taylor HE, Truini M, Rihs JR, Felger TJ (2005) Chemical characteristics of ground-water discharge at selected springs, South Rim Grand Canyon, Arizona. US Geol Surv Sci Invest Rep 04-5146
- Natural Resources Conservation Service (NRCS), USDA (2021) Bright Angel Station, Az, 12N01, SNOTEL, snow depth data. www.wcc. nrcs.usda.gov. Accessed September 2022

- Parkhurst D (1995) Users guide to PHREEQC: a computer program for speciation, reaction-path, advective-transport, and inverse geochemical calculations. USGS, Reston, VA
- Piper AM (1944) A graphic procedure in the geochemical interpretation of water-analyses. Eos Trans AGU 25:914–928. https://doi.org/10.1029/TR025i006p00914
- Sharp (2007) Principles of stable isotope geochemistry. Prentice Hall, Upper Saddle River, NJ
- Solder JE, Beisner KR (2020) Critical evaluation of stable isotope mixing end-members for estimating groundwater recharge sources: case study from the South Rim of the Grand Canyon, Arizona, USA. Hydrogeol J. https://doi.org/10.1007/s10040-020-02194-y
- Solder J, Beisner KR, Anderson J, Bills DJ (2020) Rethinking ground-water flow on the South Rim of the Grand Canyon, USA: characterizing recharge sources and flow paths with environmental tracers. Hydrogeol J 28:1593–1613. https://doi.org/10.1007/s10040-020-02193-z
- Tillman FD, Gangopadhyay S, Pruitt T (2020) Recent and projected precipitation and temperature changes in the Grand Canyon area with implications for groundwater resources. Sci Rep 10(1):1–11. https://doi.org/10.1038/s41598-020-76743-6
- Tobin BW, Springer E, Kreamer DK, Schenk E (2017) Review: The distribution, flow, and quality of Grand Canyon Springs, Arizona (USA). Hydrogeol J. https://doi.org/10.1007/s10040-017-1688-8
- USGS (2006) National field manual for the collection of water-quality data. US Geol Surv Tech Water Resour Invest 09
- Wassenaar LI, Ahmad M, Aggarwal P, van Duren M, Pöltenstein L, Araguas L, Kurttas T (2012) Worldwide proficiency test for routine analysis of δ²H and δ¹⁸O in water by isotope-ratio mass spectrometry and laser absorption spectroscopy. Rapid Commun Mass Spectrom 26:1641–1648. https://doi.org/10.1002/rcm.6270
- Woodhouse CA, Meko DM, MacDonald GM, Stahle DW, Cook ER (2010) A 1,200-year perspective of 21st century drought in southwestern North America. PNAS 107(50):21283–21288

Publisher's note Springer Nature remains neutral with regard to jurisdictional claims in published maps and institutional affiliations.

